

Article

Mass Deposition Fluxes of Asian Dust to the Bohai Sea and Yellow Sea from Geostationary Satellite MTSAT: A Case Study

Qianguang Tu ^{1,2}, Zengzhou Hao ^{1,*} and Delu Pan ^{1,2}

¹ State Key Laboratory of Satellite Ocean Environment Dynamics, Second Institute of Oceanography, State Oceanic Administration, Hangzhou 310012, China; E-Mails: thotho@163.com (Q.T.); pandelu@sio.org.cn (D.P.)

² Department of Earth Sciences, Zhejiang University, Hangzhou 310027, China

* Author to whom correspondence should be addressed; E-Mail: hzyx80@sio.org.cn (Z.H.); Tel.: +86-571-8196-3121; Fax: +86-571-8196-3121.

Academic Editor: Robert W. Talbot

Received: 4 September 2015 / Accepted: 10 November 2015 / Published: 18 November 2015

Abstract: Windblown dust aerosol plays an important role in marine ecosystems once they are deposited and dissolved. At present, methods for estimating the deposition flux are mainly limited to direct measurements or model outputs. Additionally, satellite remote sensing was often used to estimate the integral dust column concentration (DCC). In this paper, an algorithm is developed to estimate the mass deposition fluxes of Asian dust by satellite. The dust aerosol is identified firstly and then the DCC is derived based on the relationships between the pre-calculated lookup table (LUT) and observations from Japanese geostationary Multi-functional Transport Satellites (MTSAT). The LUT is built on the dust cloud and surface parameters by a radiation transfer model Streamer. The average change rate of deposition is derived, which shows an exponential decay dependence on transport time along the pathway. Thus, the deposition flux is acquired via integrating the hourly deposition. This simple algorithm is applied to a dust storm that occurred in the Bohai Sea and Yellow Sea from 1 to 3 March 2008. Results indicate that the properties of the dust cloud over the study area changed rapidly and the mass deposition flux is estimated to be 2.59 Mt.

Keywords: dust aerosol; mass deposition flux; remote sensing; MTSAT; the Bohai Sea and Yellow Sea

1. Introduction

Dust aerosol carried by dust storm events from Asia not only damage to the local ecosystems and human society, but also have large impacts on downwind areas such as Japan, Korea, and even the West Pacific Ocean through long-range transport [1]. Dust aerosol in the atmosphere play an important role in the radiative forcing of the atmosphere via scattering and absorbing shortwave and longwave radiation [2]. Once deposited and dissolved in the ocean, it modifies biogeochemistry and carbon export [3]. Especially in the high nutrient low chlorophyll (HNLC) open ocean regions, the availability of iron is the limiting factor for phytoplankton growth [4]. It is reported that direct bio-available soluble iron occupies 0.01%–80% of the dust aerosol [5]. The deposition fluxes of particulate Fe and P during the dust storm events associated with precipitation were about 500–1000 times of the daily averaged flux during non-dust days [6]. Tan and Wang [7] found that the iron deposited by the severe dust episode could have increased the chlorophyll a concentration in the southern Yellow Sea by 10%–68%. Yuan and Zhang [8] also showed a strong correlation between the dust events and biological productivity through the oceanic sediment-trap substances. However, significant uncertainties still remain in understanding the whole dust process, including generation, long-range transport, deposition, and their impact on ocean.

In this paper, we focus on the estimation of dust mass deposition fluxes over the ocean. The dust aerosol sinks into the ocean through wet and dry deposition in the transport passage. The deposition in the ocean plays an important role in the mineral dust cycle. The development of the dust deposition flux estimation methods was summarized, and they were compared to each other by Niedermeier *et al.* [9]. The dust deposition flux is mainly from direct measurements or model outputs. Each method has its own advantages and disadvantages. The direct measurement method is easy to calculate. However, the samplings are sensitive to wind erosion and other perturbations, which need to be corrected for the efficiency of the collection sampler. Furthermore, direct measurements are sparse and non-uniform, especially in the open oceans because of the prohibitive costs as well as the episodic nature of atmospheric deposition into the ocean. Therefore, various global [10,11] and regional [12,13] dust models have been developed to estimate the emissions, transport and deposition since the late 1980s. In contrast to global models, regional models provide better results with higher spatial resolution and lower uncertainties. Unfortunately, the synchronous meteorological and hydrological fields are often very scarce, which are necessary for the models. Current model estimates of mass concentrations of dust can vary from a factor of two at the global scale to at least one order of magnitude in regional model studies [14]. Sometimes, the results from different model simulations are different from each other when performing the same test [13].

On the one hand, because of the lack of continuous and simultaneous observational data, dust deposition over the ocean is still poorly understood, which badly needs quantitative evaluation research. On the other hand, satellites can provide continuous dust monitoring over large areas now and the development of inverse data calculation methods can produce quantitative estimates of dust column concentration (called dust burden or dust load). An algorithm for the retrieval of volcanic particle size and optical thickness to derive the column concentration from the Advanced Very High Resolution Radiometer (AVHRR) thermal infrared observations was developed by Wen and Rose [15]. A similar method was applied to a 7 April 2001 dust storm over northern China using the Moderate Resolution

Imaging Spectroradiometer (MODIS) data [16]. The wide spectral range of visible and near infrared technique can be used to retrieve dust load over ocean was demonstrated by Tanré *et al.* [17]. The first example of MODIS data to distinguish dust from smoke and maritime aerosols and to evaluate the African dust column concentration was shown by Kaufman *et al.* [18]. A retrieval algorithm to obtain the optical thickness, dust particle effective radius and integral dust column density simultaneous, using three MODIS thermal IR channels was developed by Zhang *et al.* [19]. Polar satellite observations are widely used to estimate the dust column concentration. However, it is insufficient to estimate the dust deposition by a snapshot of polar satellite observations as dust storms evolve with time and space rapidly.

In this study, a new algorithm is developed to estimate the deposition flux of a dust event using the geostationary satellite data. The organization of this paper is as follows. In Section 2, a brief overview of the Multifunctional Transport Satellites 1R (MTSAT-1R) data and Streamer model are provided. The detail of dust deposition flux estimation algorithm is presented in Section 3. Section 4 explains the technique applied to the dust event over the Bohai Sea and Yellow Sea from 1 to 3 March 2008. Conclusions are presented in Section 5.

2. Data and Radiative Transfer Models

2.1. Multifunctional Transport Satellites 1R (MTSAT-1R) Observations

The Multi-functional Transport Satellite 1R (hereafter MTSAT-1R) of Japan Meteorological Agency was launched on 26 February 2005. It is located 35,800 km above the equator at 140 degrees east longitude and provides wide coverage for the Pacific Ocean. MTSAT-1R carries a five-channel imager called Japanese Advanced Meteorological Imager (JAMI), providing nominal half-hourly images. JAMI consists of one visible channel and four infrared (IR) channels. The characteristics of these channels are listed in Table 1 (for more details, see [//www.jma.go.jp/jma/jma-eng/satellite/](http://www.jma.go.jp/jma/jma-eng/satellite/)).

Table 1. The characteristics of MTSAT channels.

Channel	Wavelength / μm	Quantization Levels/bit	Space Resolution /km
Visible (VIS)	0.55–0.90	10	1
Thermal IR 1 (IR1)	10.3–11.3	10	4
Thermal IR 2 (IR2)	11.5–12.5	10	4
IR water vapor (IR3)	6.5–7.0	10	4
Mid-IR (R4)	3.5–4.0	10	4

Two thermal infrared data, IR1 and IR2, are used to monitor the transport of dust storm events and quantify the depositions during the process. IR1 and IR2 of MTSAT-1R are well calibrated and show no serious systematic errors or biases with respect to the corresponding channels of MODIS [20].

2.2. Streamer

There are many radiative transfer models, such as LOW resolution TRANsmision Model (LOWTRAN), MODerate resolution atmospheric TRANsmission (MODTRAN), Second Simulation of the Satellite Signal in the Solar Spectrum (6S), and Streamer, widely used in remote sensing applications.

Streamer, which is based on plane-parallel theory, possesses the ability to simulate radiances for a variety of cloud atmospheric situations [21]. It is available freely as well as being efficient, flexible and user-friendly. In this paper, Streamer is selected to simulate the satellite radiance of dust aerosol. In Streamer simulation, each computed radiance or reflectance is done for a scene by using the discrete ordinate solver, DISORT (Discrete ordinates radiative transfer) [22]. There are seven standard atmospheric profiles in the Streamer: tropical, mid-latitude summer, mid-latitude winter, subarctic summer, subarctic winter, arctic summer and arctic winter. User-defined profiles can also be used. Dust aerosol optical and geometrical thickness, or the optical properties and phase function, may be specified as input. In addition, in order to better simulate the satellite observations, the response function of MTSAT1R is integrated into the Streamer model.

3. Methodology

According to the retrieval method of Zhang *et al.* [23], the dust optical thickness and particle size are retrieved first. Dust column density is then derived from dust optical thickness and particle size. The dust deposition is calculated based on the hourly MTSAT column dust density (Figure 1).

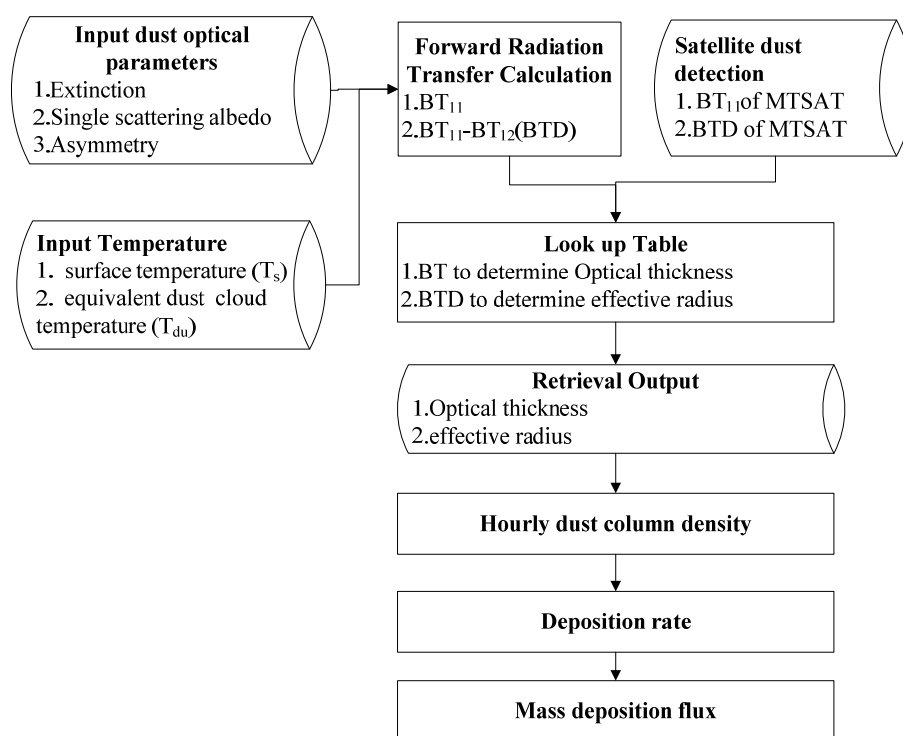


Figure 1. Flow chart of the dust deposition flux estimation process.

The basic theory and algorithm can be briefly described as follows. Satellite sensor observations, through a semitransparent dust cloud, include two parts: radiance transmitted from the underlying surface and radiance emitted from the dust cloud. This can be expressed as the following equation [15]:

$$I_i = t_i(r_e, \tau_{du}) (B(T_s) - B(T_{du})) + (1 - R_i(r_e, \tau_{du})) B(T_{du}) \tag{1}$$

where I_i is the radiance centered at wavelength λ_i , T_s is the brightness temperature of the surface, T_{du} is the equivalent temperature of the top of the cloud, B is the Planck function, t is the transmissivity, R is

the reflectivity, r_e is the effective radius of the dust, and τ_{du} is the dust optical depth. r_e and τ_{du} are defined as follows:

$$\tau_{du} = \int Q_{ext} \pi r^2 n(r) dr \tag{2}$$

$$r_e = \frac{\int \pi r^3 n(r) dr}{\int \pi r^2 n(r) dr} \tag{3}$$

where $n(r)$ is the particle size distribution, and Q_{ext} is the light extinction efficiency decided by Mie scattering. For the large size parameter of dust, the Q_{ext} is oscillating near 2. t and R are functions of r_e and τ_{du} . That is to say, r_e and τ_{du} can be retrieved simultaneously by a pair of radiances (I_i, I_j). The infrared observations of MTSAT have been transformed to brightness temperatures instead of radiance, although they can be transformed easily by Plank Law. Thus, the radiative transfer model Streamer is used to simulate the theoretical brightness temperatures at various dust cloud and surface parameters with specific aerosol physical parameters. The aerosol physical parameters, such as the single scattering albedo, asymmetry factor, and extinction coefficient ratio of the dust layer, are calculated first by Mie scattering theory based on several assumptions [24]. These assumptions are: (1) dust particles are spherical; (2) dust particle size distribution is lognormal; and (3) complex refractive index is calculated based on HITRAN 2008 dataset under different relative humidity conditions (0, 30%, 50%, 70%, and 95%). To simplify the calculation, we assume that the underlying surface is homogeneous and the dust aerosol is a single layer parallel to the surface. The lookup table (LUT) is calculated with seven T_s (from 265 K to 295 K in 5 K increments), seven T_{du} (from 260 K to 290 K in 5 K increments), 19 optical thicknesses (from 0.3 to 1 in 0.1 increments and 1 to 15 in increments of 1), and 29 particle effective radii (from 0.1 to 2 in 0.1 increments and 2 to 10 in increments of 1). The main input parameters used to generate the LUT are summarized in Table 2. To make the simulation more realistic, user-defined atmospheric profiles, instead of the standard atmospheric profiles, are used in Streamer. The atmospheric profiles of pressure, temperature and humidity are defined based on the sounding observations (<http://www.weather.uwyo.edu/upper air/sounding.html>) on the transport pathway during the dust event. Emissivity type is the surface emissivity control. Generally, ocean emissivity lies between 0.96 and 0.99 in infrared bands. In this study, 0.98 is chosen for infrared bands calculation. The height of the long-range transport of Asia to the China Seas were usually in heights between 0.5 km and 1.5 km [25]. According to this, the bottom height is set to 0.5 km.

Table 2. Streamer input parameters.

Parameter	Value
Atmospheric profiles	User-defined by radiosonde data
surface type	water
emissivity	0.98
Surface temperatures (K)	(265~295 (5)), bracketed text indicates step
dust temperatures (K)	(260~290 (5)), bracketed text indicates step
dust cloud bottom height (km)	0.5
optical thickness	(0.3~1.0 (0.1), 1.0~15.0 (1))
effective radius (μm)	(0.1~2.0 (0.1), 2~10 (1))

The MTSAT brightness temperatures are then compared with pre-calculated values from LUT until the best (least-squares) fit is obtained. The optical thickness τ_{du} and effective radius r_e can be retrieved from the best fit. Then, dust mass column concentration M_{du} is derived from the optical thickness and effective radius, using the following relationships between the dust mass and volume to the dust size distributions:

$$M_{du} = \frac{4\rho}{3} \int \pi r^3 n(r) dr \tag{4}$$

Combining Equations (2)–(4),

$$M_{du} = \frac{2\rho}{3} r_e \tau_{du} \tag{5}$$

Thus, the dust column density is widely estimated from polar sun synchronous satellites. However, it is insufficient to estimate the deposition from the column dust density only at a single time due to the high temporal and spatial variability, and the deposited rate is usually unknown. The continuous geostationary satellites observations with high temporal resolution provide the opportunity to estimate the ratio of deposition $\overline{v_{du}}$. The $\overline{v_{du}}$ is determined by derivative of an exponential model described in Section 4.3, which is obtained by means of regression from the selected mean dust column density $\overline{M_{du}}$ over the water. Thus, the dust deposition at time i can be estimated as follows,

$$\overline{M_{de}[i]} = \overline{M_{du}[i]} \times \overline{v_{du}[i]} \times S_{du}[i] \tag{6}$$

where S_{du} represents the cover area of the dust. The total deposition amount M_{de} is the sum of $\overline{M_{de}[i]}$ throughout the event,

$$M_{de} = \sum_{i=1}^T \overline{M_{de}[i]} \tag{7}$$

where T is the duration of the dust event, defined once the dust cloud transport to the study region until they pass through entirely.

4. Study Case

In this study, the MTSAT observation of the dust storm on 1–3 March 2008 is selected as the case for examining the dust deposition flux estimation algorithm.

4.1. Dust Detection

The dust cloud over the Bohai Sea and Yellow Sea on 1–3 March 2008 was discriminated first based on the detection algorithm developed by Tu *et al.* [26]. In the MTSAT brightness temperature difference (BTD) images (Figure 2), the strong negative BTD signals indicate the larger amounts of dust aerosol over the sea. The strong negative BTD results from the absorption effects of mineral dust. The dust aerosol was verified by the near simultaneous RGB true color composition images results from National Oceanic and Atmospheric Association (NOAA) series (Figure 3).

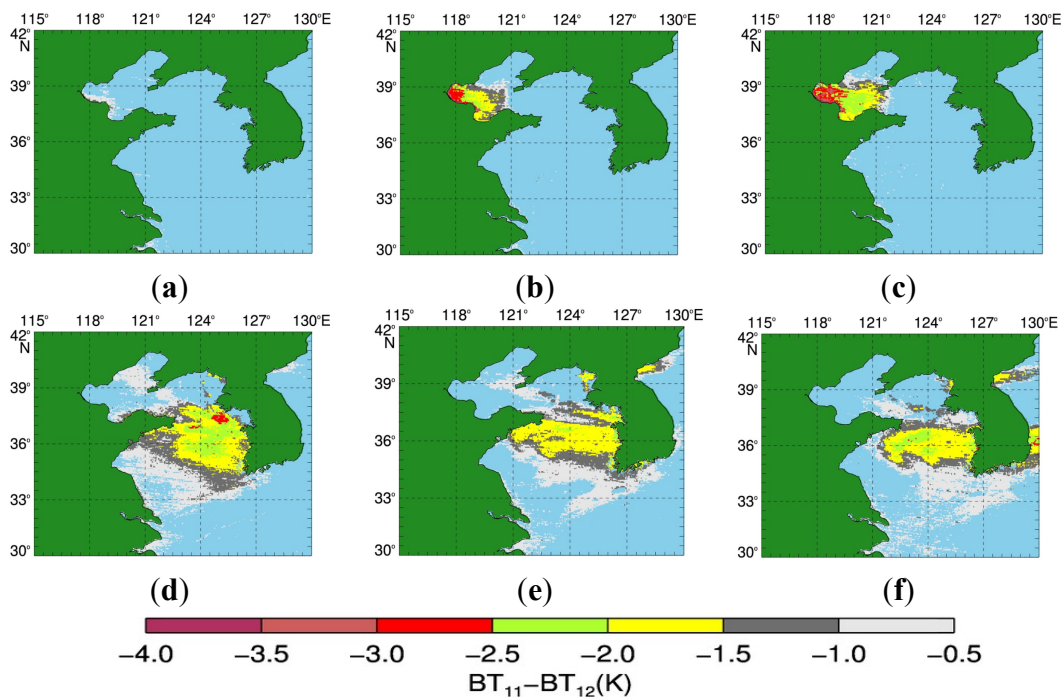


Figure 2. MTSAT brightness temperature difference (BTD) images identified the evolution of the dust event on 1–2 March 2008; (a) 200803010130; (b) 200803010530; (c) 200803010730; (d) 200803020130; (e) 200803020430; (f) 200803020730.

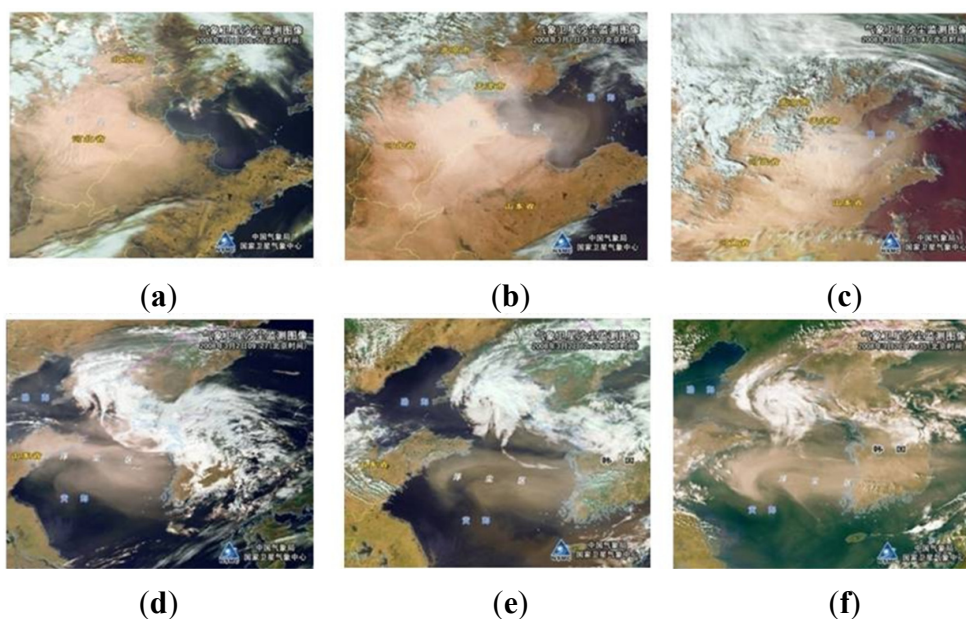


Figure 3. RGB true color composition images from the NOAA series for the comparison of the dust detection results corresponding to Figure 2; (a) 200803010150(NOAA17); (b) 200803010502(NOAA18); (c) 200803010747(NOAA16); (d) 200803020127 (NOAA17); (e) 200803020452(NOAA18); (f) 200803020735(NOAA16).

On 1 March 2008, a dust storm originated from Mongolia, spread to China over the Inner Mongolia and Loess Plateau events. Then, the evolution of the dust is indicated by the yellow color relative to the white cloud systems on true color images of the NOAA series satellites. It began entering Bohai at about

1:50 a.m., and then crossing the Bohai Sea, the Yellow Sea, and the north of the East China Sea on the following two days.

4.2. MTSAT-Derived Dust Properties Mapping and Comparison

The retrieval algorithm mentioned above was applied to the detected dust pixels. Figure 4 shows one of the Streamer simulation results when the cloud temperature and surface temperature were 260 K and 285 K, respectively.

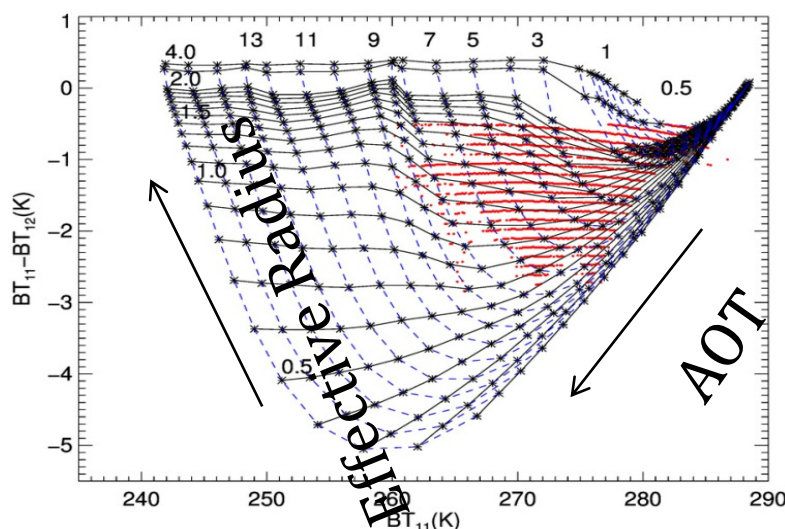


Figure 4. The BT_{11} and $BT_{11} - BT_{12}$ for individual pixel values (red dots) of MTSAT data on the Streamer simulation tables.

Any individual red dot is determined by the BT_{11} and $BT_{11} - BT_{12}$ observed from MTSAT. The black curves and the blue curves are the BT_{11} and $BT_{11} - BT_{12}$ simulated from Streamer model at different effective radii and AOTs. They are used to generate a lookup table. It can be seen that BT_{11} is almost decreasing linearly with increasing optical thickness, while $BT_{11} - BT_{12}$ decreases with an almost linear increase of particle effective radius. Since the observation of satellite is the mixture of the surface and dust cloud temperature, under a fix surface temperature, the lower BT_{11} usually means the higher altitude the dust cloud has reached. The higher altitude may correspond to heavy dust aerosol loading with higher AOT. Depending on this physical pattern, the optical thickness and particle effective radii of dust particles can be retrieved according to the position of the red dots in the grids.

Then, the dust column density can be obtained using the derived equations. The dust density may be different from different source and transport routes. The specific density for Sahara dust is reported as $\rho = 2.6 \text{ g/cm}^3$ [27]. For Asian dust, however, this value is usually taken as 2.5 g/cm^3 [16,23], which was also used in our study. Figure 5a–c shows the MTSAT retrieved results of the dust optical thickness, effective radius and column density at 2:30 a.m. on 2 March 2008. Unfortunately, the retrieval results lack robust validations with the *in situ* measurements. To further increase confidence on the performance of our algorithm, the results are compared with the MODIS retrieval at 2:05 a.m. (Figure 5d,f).

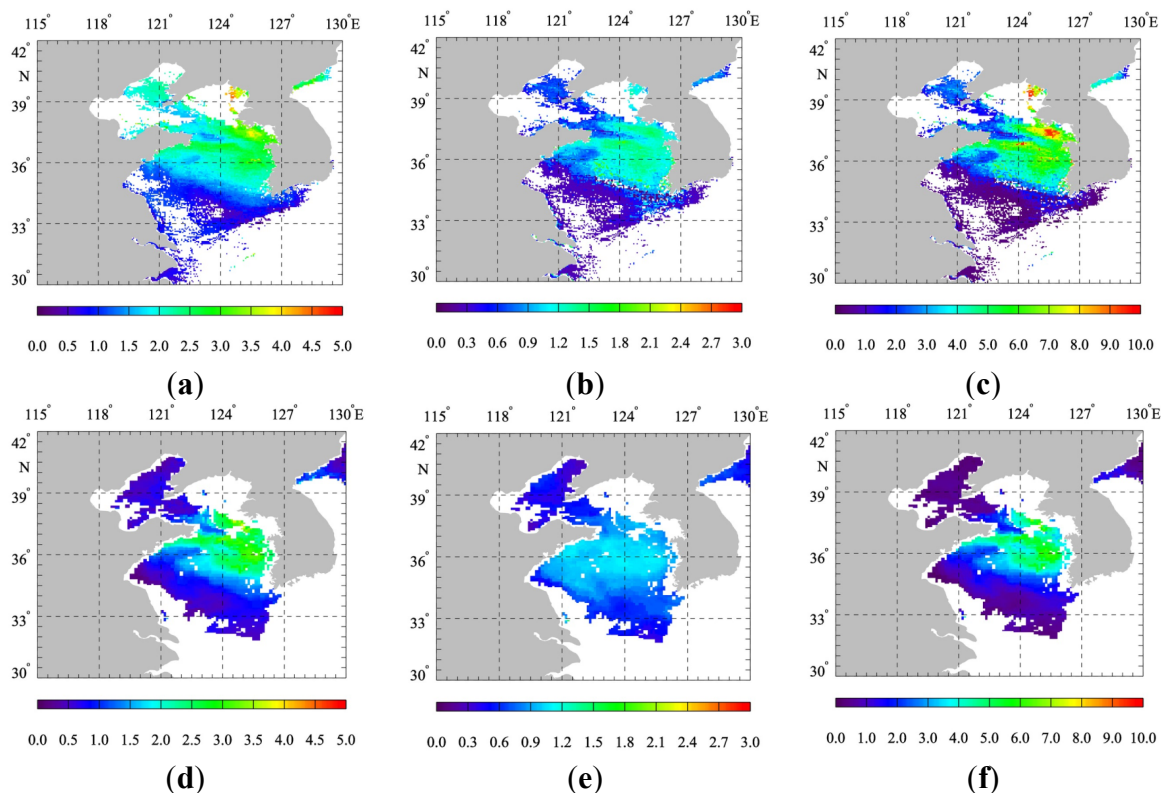


Figure 5. Comparison between MTSAT (a–c) and MODIS (d–f), retrieved at nearly simultaneous time points; (a) MTSAT AOT; (b) MTSAT effective radius; (c) MTSAT column dust density(gm^{-2}); (d) MODIS AOT; (e) MODIS effective radius; (f) MODIS column dust density(gm^{-2}).

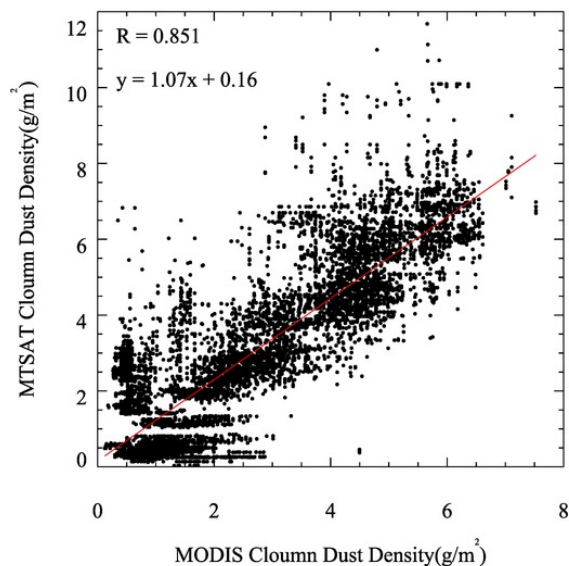


Figure 6. Correlation plots of the dust column concentrations obtained from MODIS compared to MTSAT.

Focusing on the major regions of the dust cloud, the MTSAT retrieved AOT is largely consistent with the MODIS. However, for some regions, especially the outer rim, it shows relatively large differences. This is mainly due to the rapid variations that occur in the outer rim within a short time. Moreover, the

MODIS and MTSAT retrievals should not be expected to precisely the same. The dust column density has a generally similar pattern and good correlation between MODIS and MTSAT retrievals (Figure 6).

4.3. Estimation of the Total Deposited Mass

The satellite observation is a snapshot of one scenario of the dust event. It is a comprehensive reflection of dust transport, diffusion and deposition. It is difficult to tell these processes apart from each other from the satellite. Thus, the variation of the space average of the dust column density is used to derive the deposition ratio. The horizontal transport velocities are usually much larger than the deposition velocities. To minimize the influence of horizontal transport, only the space average of the dust column density, in which a standard deviation less than a threshold is selected to build the regression model. The threshold is set to 1.5g/m² from experience. The average dust column density \overline{M}_{du} decreases exponentially with an increase of dust transport time (Figure 7). Thus, an exponential model was created from the selected \overline{M}_{du} . The regression model is shown as follows:

$$y=ae^{-bx} + c \tag{8}$$

where y is the value of mean dust column density, x is time from the dust began to enter the seas, and a, b, and c are 5.509, 0.142 and 0.35, respectively, for this case. These are regressed from the model, and the correlation coefficient between x and y is $R^2 = 0.925$. This empirical model may be limited for this case study in the Bohai Sea and the Yellow Sea and for other cases, the coefficients a, b, and c of the model $y=a \times e^{-bx} + c$ can to be regressed by our method. Further study is needed to improve the model and to make it more robust. The ratio of deposition (\overline{v}_{du}) was determined by the derivative of the exponential model

$$\overline{v}_{du[x]} = -0.782e^{-0.142x} \tag{9}$$

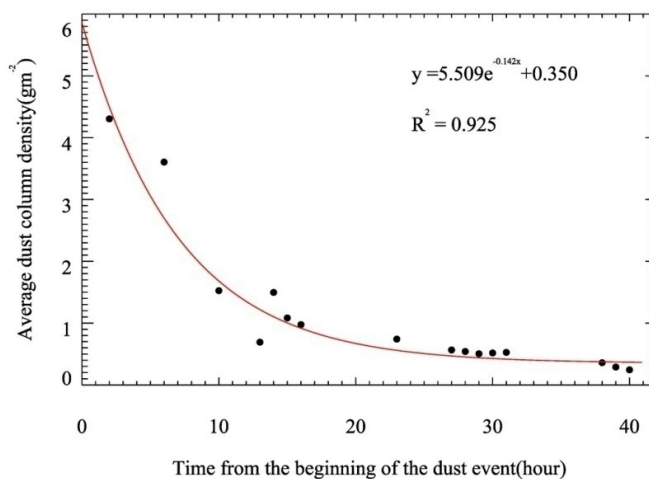


Figure 7. Variation of dust deposition rates (g/m²) with relative time from when the dust reached the Bohai Sea.

The deposition amount M_{de} for each pixel is derived using Equations (6) and (7) and the space distribution is shown in Figure 8.

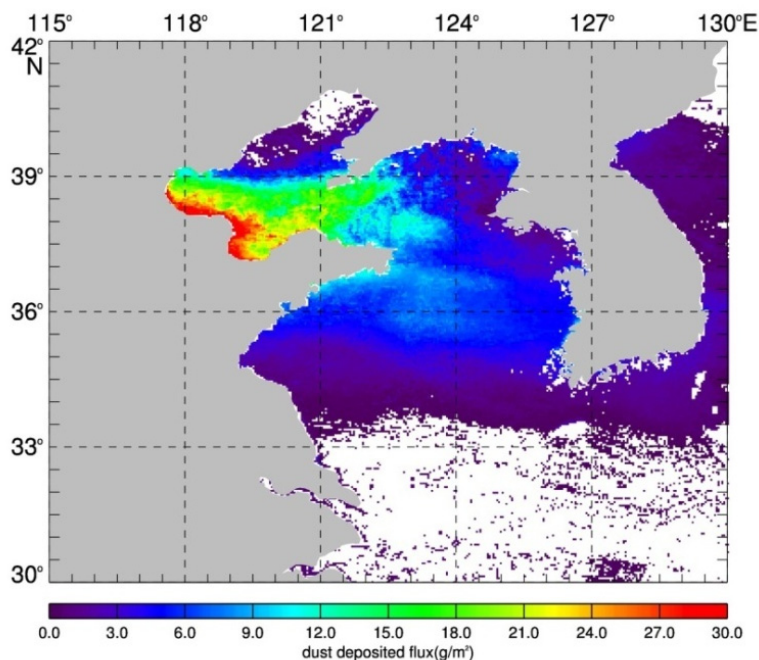


Figure 8. The spatial distribution of dust depositon during the period of 1–2 March 2008.

The coarser dust particles are removed faster than the finer ones. Therefore, total deposition flux decreased rapidly on the way from the Bohai Sea (~20 g/m²) to the Yellow Sea (~6 g/m²). Table 3 shows the annual deposition flux in the study region from previous cruise and site measurements and modeling results at different time periods. The values are vary.

Table 3. The dust deposition over the Bohai Sea and the Yellow Sea (g/m²·year).

Authors	Time Period	Methods	The Bohai Sea	The Yellow Sea
Liu and Zhou [28]	1987–1992	cruise track	26.4	9.3
Uematsu <i>et al.</i> [29]	1994–1995	model	17.5	9.7
Gao <i>et al.</i> [30]	1989	sites	30~196	8.6~79

Uematsu *et al.* [31] used four island stations to estimate the total deposition of atmospheric mineral to the central North Pacific to be ~20 Mt·yr⁻¹ from January 1981 to March 1982. Gao *et al.* [32] estimated the total atmospheric deposition of dust to the China Sea as about 67 Mt·yr⁻¹ for 1992. Kai and Huiwang [33] estimated the total amount of dry deposition to the Yellow Sea to be 17.9 Mt·yr⁻¹ from the difference between the inland city (Beijing) and the coastal city (Qingdao) samples during 2000–2002. There were five dust-transporting events in this study region based on the national sand-dust weather almanac and dust detection procedure for 2008. The total deposition amount into the Bohai Sea and the Yellow Sea during the case event was estimated to be 2.59 Mt. If the total deposition amount of this case event were multiplied by five, the magnitude would be roughly comparable to previous *in situ* and model results. The values are varied because the intensity and duration of the dust events change greatly over time and space as well as the estimating methods were different.

5. Conclusions

This study provides an alternative method to estimate the deposition flux of dust aerosol over the seas from geostationary satellites. The MTSAT observations are used to investigate a dust event over the Bohai Sea and the Yellow Sea during 1–3 March 2008. The major conclusions are as follows: (1) Streamer is suitable to simulate the brightness temperature and the simulations can be used to create the LUT under different conditions; (2) spatial mapping of retrievals of the dust clouds with MTSAT agrees with nearly synchronous MODIS products and the correlation of dust column concentration reaches 0.85; (3) the dust column concentration decreased exponentially with the dust transport time on the pathway; and (4) the magnitude of the deposition flux is comparable to the *in situ* and model results from previous studies.

This paper demonstrates that two-band MTSAT retrievals of dust events could be used to routinely quantify the deposition of dust storm events over the seas under reasonable assumptions. These methods can be used to create a long-term time series of dust deposition flux in the coastal seas of China. The satellite estimated deposition flux would be a direct index for investigating the biogeochemical implications in this area for further study.

Acknowledgments

We thank the three anonymous reviews' advice to improve this paper significance. This material is based upon work funded by the National Natural Science Foundation of China (No. 41476157), the National Natural Science Youth Foundation of China (No. 40806071) and the Project of State Key Laboratory of Satellite Ocean Environment Dynamics, Second Institute of Oceanography (No. SOEDZZ1515).

Author Contributions

Tu Qianguang, Hao Zengzhou, and Pan Delu designed the basic lines of the study. All the authors contributed equally to this work.

Conflicts of Interest

The authors declare no conflict of interest.

References

1. Mikami, M.; Shi, G.Y.; Uno, I.; Yabuki, S.; Iwasaka, Y.; Yasui, M.; Aoki, T.; Tanaka, T.Y.; Kurosaki, Y.; Masuda, K.; *et al.* Aeolian dust experiment on climate impact: An overview of japan-china joint project adec. *Global Planet. Change* **2006**, *52*, 142–172.
2. Sokolik, I.N.; Winker, D.M.; Bergametti, G.; Gillette, D.A.; Carmichael, G.; Kaufman, Y.J.; Gomes, L.; Schuetz, L.; Penner, J.E. Introduction to special section: Outstanding problems in quantifying the radiative impacts of mineral dust. *J. Geophys. Res. -Atmos.* **2001**, *106*, 18015–18027.
3. Tagliabue, A.; Aumont, O.; Bopp, L. The impact of different external sources of iron on the global carbon cycle. *Geophys. Res. Lett.* **2014**, *41*, 920–926.

4. Jickells, T.D.; An, Z.S.; Andersen, K.K.; Baker, A.R.; Bergametti, G.; Brooks, N.; Cao, J.J.; Boyd, P.W.; Duce, R.A.; Hunter, K.A.; *et al.* Global iron connections between desert dust, ocean biogeochemistry, and climate. *Science* **2005**, *308*, 67–71.
5. Mahowald, N.M.; Baker, A.R.; Bergametti, G.; Brooks, N.; Duce, R.A.; Jickells, T.D.; Kubilay, N.; Prospero, J.M.; Tegen, I. Atmospheric global dust cycle and iron inputs to the ocean. *Global Biogeochem. Cycles* **2005**, doi:10.1029/2004GB002402.
6. Shi, J.-H.; Zhang, J.; Gao, H.-W.; Tan, S.-C.; Yao, X.-H.; Ren, J.-L. Concentration, solubility and deposition flux of atmospheric particulate nutrients over the yellow sea. *Deep-Sea Res. Part II-Topical Stud. in Oceanogr.* **2013**, *97*, 43–50.
7. Tan, S.-C.; Wang, H. The transport and deposition of dust and its impact on phytoplankton growth in the yellow sea. *Atmos. Environ.* **2014**, *99*, 491–499.
8. Yuan, W.; Zhang, J. High correlations between asian dust events and biological productivity in the western north pacific. *Geophys. Res. Lett.* **2006**, doi:10.1029/2005GL025174.
9. Niedermeier, N.; Held, A.; Muller, T.; Heinold, B.; Schepanski, K.; Tegen, I.; Kandler, K.; Ebert, M.; Weinbruch, S.; Read, K.; *et al.* Mass deposition fluxes of saharan mineral dust to the tropical northeast atlantic ocean: An intercomparison of methods. *Atmos. Chem. Phys.* **2014**, *14*, 2245–2266.
10. Ginoux, P.; Chin, M.; Tegen, I.; Prospero, J.M.; Holben, B.; Dubovik, O.; Lin, S.J. Sources and distributions of dust aerosols simulated with the gocart model. *J. Geophys. Res. -Atmos.* **2001**, *106*, 20255–20273.
11. Zender, C.S.; Bian, H.S.; Newman, D. Mineral Dust Entrainment and Deposition (DEAD) model: Description and 1990s dust climatology. *J. Geophys. Res. -Atmos.* **2003**, doi:10.1029/2002JD002775.
12. Wang, Z.F.; Ueda, H.; Huang, M.Y. A deflation module for use in modeling long-range transport of yellow sand over east asia. *J. Geophys. Res. -Atmos.* **2000**, *105*, 26947–26959.
13. Uno, I.; Carmichael, G.R.; Streets, D.G.; Tang, Y.; Yienger, J.J.; Satake, S.; Wang, Z.; Woo, J.H.; Guttikunda, S.; Uematsu, M.; *et al.* Regional chemical weather forecasting system cfors: Model descriptions and analysis of surface observations at japanese island stations during the ace-asia experiment. *J. Geophys. Res. -Atmos.* **2003**, doi:10.1029/2002JD002845.
14. Huneus, N.; Schulz, M.; Balkanski, Y.; Griesfeller, J.; Prospero, J.; Kinne, S.; Bauer, S.; Boucher, O.; Chin, M.; Dentener, F.; *et al.* Global dust model intercomparison in aerocom phase i. *Atmos. Chem. Phys.* **2011**, *11*, 7781–7816.
15. Wen, S.; Rose, W.I. Retrieval of sizes and total masses of particles in volcanic clouds using AVHRR bands 4 and 5. *J. Geophys. Res.* **1994**, *99*, 5421–5421.
16. Gu, Y.; Rose, W.I.; Bluth, G.J.S. Retrieval of mass and sizes of particles in sandstorms using two MODIS IR bands: A case study of April 7, 2001 sandstorm in China. *Geophys. Res. Lett.* **2003**, doi:10.1029/2003GL017405.
17. Tanre, D.; Kaufman, Y.J.; Herman, M.; Mattoo, S. Remote sensing of aerosol properties over oceans using the modis/eos spectral radiances. *J. Geophys. Res. -Atmos.* **1997**, *102*, 16971–16988.
18. Kaufman, Y.J.; Koren, I.; Remer, L.A.; Tanre, D.; Ginoux, P.; Fan, S. Dust transport and deposition observed from the terra-moderate resolution imaging spectroradiometer (MODIS) spacecraft over the atlantic ocean. *J. Geophys. Res. -Atmos.* **2005**, doi:10.1029/2003JD004436.
19. Zhang, P.; Lu, N.; Hu, X.; Dong, C. Identification and physical retrieval of dust storm using three modis thermal ir channels. *Global Planet. Change* **2006**, *52*, 197–206.

20. Sohn, B.J.; Park, H.S.; Han, H.J.; Ahn, M.H. Evaluating the calibration of MTSAT-1R infrared channels using collocated Terra MODIS measurements. *Int. J. Remote Sens.* **2008**, *29*, 3033–3042.
21. Key, J. *Streamer User's Guide*; Cooperative Institute for Meteorological Satellite Studies, University of Wisconsin: Wisconsin, WI, USA, 2001.
22. Stamnes, K.; Tsay, S.C.; Wiscombe, W.; Jayaweera, K. Numerically stable algorithm for discrete-ordinate-method radiative-transfer in multiple-scattering and emitting layered media. *Appl. Opt.* **1988**, *27*, 2502–2509.
23. Zhang, P.; Lu, N.; Hu, X.; Dong, C. Identification and physical retrieval of dust storm using three modis thermal ir channels. *Global Planet. Change* **2006**, *52*, 197–206.
24. Hao, Z.; Gong, F.; Pan, D.; Huang, H. Scattering and polarization characteristics of dust aerosol particles. *Acta Optica Sin.* **2012**, doi:10.3788/aos201232.0101002.
25. Lin, T.-H. Long-range transport of yellow sand to taiwan in spring 2000: Observed evidence and simulation. *Atmos. Environ.* **2001**, *35*, 5873–5882.
26. Tu, Q.; Hao, Z.; Pan, D.; Gong, F. Dust automatic detection over ocean using MTSAT data. *Acta Optica Sin.* **2011**, doi:10.3788/AOS201131.1228001.
27. Haywood, J.; Francis, P.; Osborne, S.; Glew, M.; Loeb, N.; Highwood, E.; Tanré, D.; Myhre, G.; Formenti, P.; Hirst, E. Radiative properties and direct radiative effect of Saharan dust measured by the C-130 aircraft during SHADE: 1. Solar spectrum. *J. Geophys. Res.: Atmos. (1984–2012)* **2003**, doi:10.1029/2002JD002687.
28. Liu, Y.; Zhou, M.; Atmospheric input of aerosols to the eastern seas of China. *Acta Oceanolog. Sin.* **1999**, *5*, 38–45.
29. Uematsu, M.; Wang, Z.; Uno, I. Atmospheric input of mineral dust to the western north pacific region based on direct measurements and a regional chemical transport model. *Geophys. Res. Lett.* **2003**, doi:10.1029/2002GL016645.
30. Gao, Y.; Arimoto, R.; Duce, R.; Lee, D.; Zhou, M. Input of atmospheric trace elements and mineral matter to the yellow sea during the spring of a low-dust year. *J. Geophys. Res.: Atmos. (1984–2012)* **1992**, *97*, 3767–3777.
31. Uematsu, M.; Duce, R.A.; Prospero, J.M. Deposition of atmospheric mineral particles in the north pacific ocean. *J. Atmos. Chem.* **1985**, *3*, 123–138.
32. Gao, Y.; Arimoto, R.; Duce, R.A.; Zhang, X.Y.; Zhang, G.Y.; An, Z.S.; Chen, L.Q.; Zhou, M.Y.; Gu, D.Y. Temporal and spatial distributions of dust and its deposition to the china sea. *Tellus Ser. B-Chem. Phy. Meteorol.* **1997**, *49*, 172–189.
33. Kai, Z.; Huiwang, G. The characteristics of asian-dust storms during 2000–2002: From the source to the sea. *Atmos. Environ.* **2007**, *41*, 9136–9145.